Modern Physics Letters B, Vol. 23, No. 3 (2009) 233–236

World Scientific
www.worldscientific.com

NUMERICAL SIMULATION OF SHOCK WAVE AND TURBULENCE INTERACTION OVER A CIRCULAR CYLINDER

CHANG-YUE XU, LI-WEI CHEN and XI-YUN LU*

Department of Modern Mechanics, University of Science and Technology of China, Hefei, Anhui 230026, P. R. China
**xlu@ustc.edu.cn*

Received 1 June 2008

The interaction of shock wave and turbulence for transonic flow over a circular cylinder is investigated using detached-eddy simulation (DES). Several typical cases are calculated for free-stream Mach number M_∞ from 0.85 to 0.95, and the physical mechanisms relevant to the shock wave and turbulence interaction are discussed. Results show that there exist two flow states. One is unsteady flow state with moving shock waves interacting with turbulent flow for $M_\infty < 0.9$ approximately, and the other is quasi-steady flow with stationary shocks standing over the wake of the cylinder for $M_\infty > 0.9$, suppressing the vortex shedding from the cylinder. Moreover, local supersonic zones are identified in the wake of the cylinder and generated by two processes, i.e., reverse flow and shock wave distortion induced the supersonic zone. Turbulent shear layer instabilities are revealed and associated with moving shock wave and traveling pressure wave.

Keywords: Detached eddy simulation (DES); transonic flow; shock wave; turbulent flow.

1. Introduction

The prediction of compressible flow with shock wave and turbulence interaction is a challenging problem and plays an important role in applications and fundamentals. Usually, transonic flow over a body, e.g., airfoil and cylinder, is a typical problem for studying shock wave and turbulent flow interaction[1,2]. Here, we will deal with the transonic flow past a circular cylinder to reveal the relevant physical mechanisms. Some typical work on this subject has been performed experimentally and numerically[3-6]. Compared with transonic flow past an airfoil[7,8], the flow structures of transonic flow past the cylinder become more complicated since massively separated flow occurs in the wake of the cylinder. Thus, it is still highly desirable to reveal the flow behaviors, e.g., the turbulent shear layer instability, local supersonic zone, and pressure wave traveling.

In the present study, a detached-eddy simulation (DES) is used in solving the two-dimensional (2D) Reynolds-averaged Navier-Stokes equations. Some work on flow past a cylinder has exhibited that the results predicted by the 2D simulation are well consistent with those obtained by the three-dimensional (3D) calculation[9]. Recently, a 2D DES has been successfully employed to predict the flow behaviors in a combustor[10]. Thus, we will reveal the physical mechanisms associated with the shock wave and turbulence interaction based on the 2D DES.

2. Mathematical Formulation and Numerical Methods

The Reynolds-averaged Navier-Stokes equations under the generalized coordinates are used here and normalized by the free-stream variables and the diameter of the cylinder. For neatness, the detailed formulations of the equations are not shown here and can be found in Ref. 11. The equations are numerically solved by a finite-volume method. The convective terms are discretized by a modified second-order central/upwind hybrid scheme, and the viscous terms by a second-order central difference. Time advancement is performed by an implicit approximate-factorization method with sub-iterations.

In the calculations, the initial conditions are set as the free-stream variables. The far boundary conditions are treated by locally one-dimensional Riemann-invariants. No-slip and adiabatic conditions are applied on the cylinder surface.

In this study, computational parameters are selected as follows. The free-stream Mach number M_∞ ranges from 0.85 to 0.95. The Reynolds number based on the diameter and the free-stream quantities is 2×10^5. The outer boundary of the computational domain lays at 50 times diameter and O-type grid is used with the grid number 593×593 in the radial and azimuthal direction, respectively. Time step is 0.005. Based on extensive tests, it is verified that the code used can reliably predict the flow behaviors and the computed results are independent of the time step, grid size and computational domain.

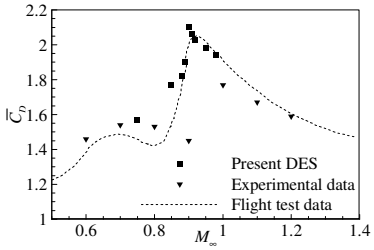

Fig. 1. Mean drag coefficient versus the Mach number.

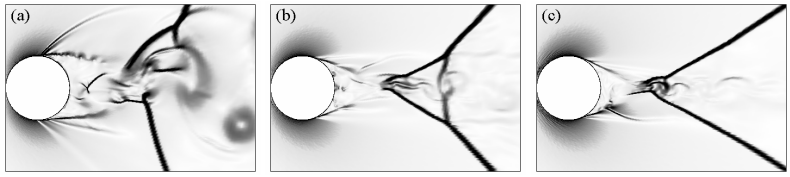

Fig. 2. Instantaneous patterns of the amplitude of density gradient: (a) M_∞ = 0.88; (b) 0.9; and (c) 0.95.

3. Results and Discussion

Some typical results are presented to discuss the flow behaviors, e.g., unsteady and quasi-steady flow state, local supersonic zone and turbulent shear layer instability. The time-averaged drag coefficient is shown in Fig. 1. It is seen that a peak of the drag coefficient occurs at M_∞ = 0.9 approximately, corresponding to the critical Mach number for dividing unsteady and quasi-steady flow regime discussed below. To validate the

present calculation, the experimental and flight test data[3,12] are also exhibited in Fig. 1 and are in good agreement with our computed results.

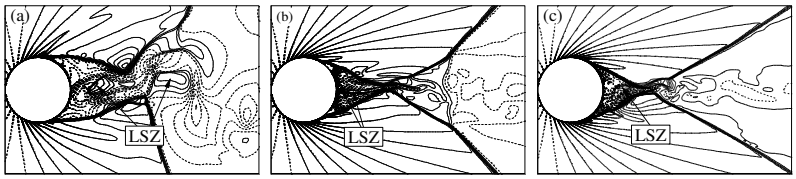

Fig. 3. Local Mach number iso-lines: (a) M_∞ = 0.88; (b) 0.9; and (c) 0.95. Here, solid lines represent $M > 1$ and dashed lines $M < 1$.

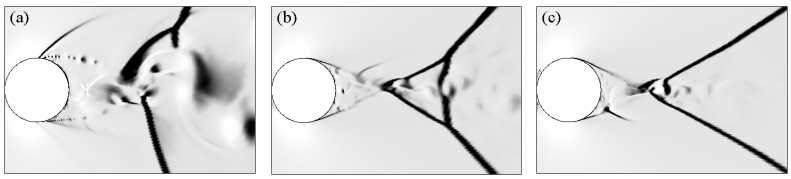

Fig. 4. Instantaneous patterns of $\partial\rho / \partial x$: (a) M_∞ = 0.88; (b) 0.9; and (c) 0.95.

Based on our results, we have identified two typical flow states, i.e., unsteady and quasi-steady flow state. To exhibit both the flow states, instantaneous Schlieren-type visualization in terms of the amplitude of density gradient $|\nabla\rho|$ is shown in Fig. 2 for three typical Mach numbers. Here, only the upper-side half flow pattern is analyzed for clearly describing the flow behavior. When M_∞ < 0.9, e.g., M_∞ = 0.88 in Fig. 2(a), corresponding to the unsteady flow state, a moving shock wave over the cylinder induces a separated shear layer and another shock wave interacts with the wake to form complex structures including secondary shock waves and large-scale vortices in the downstream of the cylinder. When M_∞ > 0.9, e.g., M_∞ = 0.95 in Fig. 2(c), corresponding to the quasi-steady flow state, a stationary shock wave is formed behind the cylinder and very weak vortical flow occurs in the downstream of the shock wave. Moreover, Fig. 2(b) shows the flow pattern for M_∞ = 0.9. The shock wave interacts with the wake to form a shock stem and a triple point. Moreover, based on the curve of time-dependent drag coefficient at M_∞ = 0.9 (not shown here), we have noticed that both the smooth curve in one period (i.e., quasi-steady flow) and oscillating variation in another period (i.e., unsteady flow) switch with each other. It is identified that M_∞ = 0.9 corresponds to the critical Mach number M_∞^c, associated with the peak value of the drag force in Fig. 1. In addition, Murthy and Rose[3] performed an experimental visualization on transonic flow past a cylinder, and found that the flow becomes quasi-steady state when M_∞ is over a critical value and vortex shedding behind the cylinder is hardly detected. Thus, the present results are well consistent with the experimental observation.

By examining the flow structures, local supersonic zone (LSZ) is reasonably detected in the wake of the cylinder. After carefully checking the animation of flow structure, we have found that there exist two processes to form the LSZ, i.e., reverse flow and shock

wave distortion. Figure 3 shows the instantaneous local Mach number iso-lines. As shown in Fig. 3(a) for M_∞ = 0.88, two LSZs occur and correspond to both the processes, respectively. The LSZ in the recirculation region behind the cylinder is induced by the reverse flow from supersonic zone interacting with the vortical flow shed from the cylinder. Similar to this process, the LSZs for M_∞ = 0.9 and 0.95 occur in Figs. 3(b) and (c). Another LSZ in the downstream of the moving shock is formed by the distorted shock wave. As the oblique shock wave is distorted due to interacting with the wake and moves upstream to form a normal-type shock wave, supersonic flow behind the oblique shock occurs and further separates from the normal shock to form a LSZ.

Turbulent shear layer instabilities are observed and induced by moving shock wave and traveling pressure wave, corresponding to the two flow states discussed above. As exhibited in Fig. 4, the streamwise derivative of density is used to show the shear layer instability processes. From Fig. 4(a) for M_∞ = 0.88 lying in the unsteady flow regime, since the moving shock wave interacts with the boundary layer, a separated shear layer is generated and evolved downstream with small-scale eddies due to the Kelvin-Helmoholtz instability. Corresponding to the quasi-steady state flow, as the interaction of the reserve flow and vortical flow in the recirculation region behind the cylinder, a pressure wave is induced, as shown in Figs. 4(b) and (c) for M_∞ = 0.9 and 0.95, and interacts with the shear layer when traveling downstream, resulting in the shear layer rolling up.

Acknowledgments

This work was supported by the National Natural Science Foundation of China (Nos. 90405007 and 90605005), Program for Changjiang Scholars and Innovative Research Team in University, and the Fund for Foreign Scholars in University Research and Teaching Programs.

References

1. H. Tijdeman and R. Seebass, *Ann. Rev. Fluid Mech*. **12** (1980) 181.
2. B. H. K. Lee, *Prog. Aerosp. Sci.* **37** (2001) 147.
3. V. S. Murthy and W. C. Rose, *AIAA J.* **16** (1978) 549.
4. O. Rodriguez, *AIAA J*. **22** (1984) 1713.
5. M. Pandolfi and F. Larocca, *Comput. Fluids*. **17** (1989) 205.
6. N. Botta, *J. Fluid Mech*. **301** (1995) 225.
7. S. Deck, *AIAA J*. **43** (2005) 1556.
8. R. Bourguet and M. Braza, *Phys. Fluids*. **19** (2007) 111701.
9. R. Mittal and S. Balachandar, *Phys. Fluids*. **7** (1995) 1841.
10. J. Y. Choi, F. Ma and V. Yang, *Proc. Combust. Inst*. **30** (2005) 2851.
11. X. Y. Lu, S. W. Wang, H. G. Sung, S. Y. Hsieh and V. Yang, *J. Fluid Mech*. **527** (2005) 171.
12. C. J. Welsh, *NACA TN 2941* (1953).